AIP | Journal of Applied Physics

Relaxor behavior in multiferroic BiMn2O5 ceramics

I. Fier, L. Walmsley, and J. A. Souza

Citation: J. Appl. Phys. **110**, 084101 (2011); doi: 10.1063/1.3650455
View online: http://dx.doi.org/10.1063/1.3650455
View Table of Contents: http://jap.aip.org/resource/1/JAPIAU/v110/i8
Published by the AIP Publishing LLC.

Relaxor behavior in multiferroic $BiMn_2O_5$ ceramics

I. Fier,[1] L. Walmsley,[1,a)] and J. A. Souza[2]
[1]*Departamento de Física, Instituto de Geociências e Ciências Exatas, Unesp Rio Claro, SP 13506-900, Brazil*
[2]*Centro de Ciências Naturais e Humanas, Universidade Federal do ABC, Santo André - SP 09090-900, Brazil*

(Received 7 April 2011; accepted 3 September 2011; published online 17 October 2011)

In polycrystalline $BiMn_2O_5$, a broad thermal stimulated depolarization current curve has been observed in the range from 10 K to 300 K and the pyroelectric coefficient determined. In magnetic susceptibility measurements reported in the literature, features appearing in the pyroelectric coefficient could also be identified for the same temperatures, suggesting a connection between electric and magnetic data above the Néel temperature. A detailed study of the dielectric constant from 240 K to 700 K for an extended range of frequencies revealed a broad maximum at low frequencies, characteristic of relaxor ferroelectrics, following Vogel-Fulcher relation. A freezing temperature of the polar nanoregions $T_f = 512$ K has been determined. This high temperature ferroelectric behavior is attributed to the Bi^{3+} in the distorted BiO_8 cage. © *2011 American Institute of Physics*. [doi:10.1063/1.3650455]

I. INTRODUCTION

In RMn_2O_5 (R = Y, Er, Tm, Tb, Gd, Dy, Ho, and Bi), the coupling between the ferroelectric and antiferromagnetic phases, with the Néel temperature ($T_N = 40$ K), and the ability of a magnetic field to change the electric polarization have been extensively studied using different techniques. Thus, most of the studies in these materials focus on the range of temperatures below 50 K. A transition from a ferroelectric to a paraelectric phase has been identified very close to the Néel temperature ($T_N = 40$ K) of the antiferromagnetic phase transition in single crystals of RMn_2O_5 by measuring dielectric constant and electrical polarization when the electric field is applied along the b-axis direction. Examples of such transitions are found along the b-axis in $TbMn_2O_5$, $DyMn_2O_5$, and $HoMn_2O_5$ compounds.[1,2] Evidences of ferroelectricity from pyroelectric current measurements have also been reported by Inomata and Kohn[3] in $GdMn_2O_5$. A peak in the dielectric constant with the applied electric field parallel to the b-axis has been seen around 40 K by Noda *et al.*[4] in RMn_2O_5 (R = Y, Er, Tm, and Ho). For a $BiMn_2O_5$ single crystal, Kim *et al.*[5] have observed a small maximum in the dielectric constant, with the electric field applied parallel to the b-axis around 40 K, and polarization for the same direction has been seen to increase from 40 K to about 0.66 K. The dielectric constant and the electrical polarization have also been investigated by applying the electric field along the c- and a-axis directions. In $TmMn_2O_5$ (Ref. 6) and $YbMn_2O_5$ (Ref. 7), a polarization flop from b- to a-axis was discovered around 5 K. Coexistence of polarization along the a- and c-axis directions has been reported by Noda *et al.*[8] in $Eu_{0.595}Y_{0.405}Mn_2O_5$. Polarization with the electric field applied along the a-axis and the magnetic field applied along the c-axis has been observed in $Eu_{0.75}Y_{0.25}Mn_2O_5$.[9] In all these studies, the measurements have been performed in a range of temperatures below 50 K, except those of Ref. 3, in which pyroelectric currents have been recorded in the range 4.2 K to 273 K.

The peak along the b-axis in the dielectric constant close to the antiferromagnetic transition temperature (40 K) has been interpreted as a ferroelectric to paraelectric phase transition. In view of the fact that, in the range 40 K–50 K, no b-axis polarization has been observed and due to the observed connection between the antiferromagnetic and ferroelectric orders,[10,11] most of the authors have assumed that the paraelectric phase of the RMn_2O_5 begins around 40 K. However, measurements of pyroelectric effect in the range 77 K–500 K using single crystals of $BiMn_2O_5$ with the applied electric field along the a-axis direction were reported by Zhitomirskii *et al.*[12] For the measured temperature range, the authors did not find any polarization along the b-axis, which is not in contradiction with the other measurements reported in the literature, since they have started their measurements at 77 K.

In the present work, we show the pyroelectric coefficient of a $BiMn_2O_5$ polycrystalline sample that has been poled at room temperature by applying an electric field of 1.8 kV/cm. The experiment was performed in the range from 10 K to 300 K, with a depolarization current being measured in the whole temperature range of the experiment. The behavior of the dielectric constant measured for several frequencies is also discussed in the low-T (10 K–216 K) and high-T (240 K–700 K) ranges. In the latter case, a detailed study as a function of the frequency was performed. The dielectric constant exhibits a frequency dependent broad maximum, following the Vogel-Fulcher relation at low frequencies, characteristic of relaxor ferroelectrics.

II. EXPERIMENTAL

A polycrystalline $BiMn_2O_5$ sample was prepared by mixing stoichiometric amounts of Bi and Mn acetates in distilled water and a 50 mol% excess of citric acid and ethylene glycol. The solution was heated at 120 °C, stirred until a gel was formed, and then dried. The organic material was oxidized for 24 h at 500 °C. The powder was ground in an agate

a)Author to whom correspondence should be addressed. Electronic mail: walmsley@rc.unesp.br.

mortar for 30 min, heat treated for 30 h at 900 °C, ground for 30 min, and heat treated again for 30 h at 1000 °C. Finally, the powder was ground for 30 min, pressed into pellets, and reacted for 30 h at 1100 °C. A detailed structural characterization is given in Ref. 13. The obtained pellets were 440 μm thick and 3 mm in diameter. Impedance spectra were obtained in a Solartron 1260 A impedance analyzer. Two different cryostats were used, Janis CCS-150 for the range 10 K–325 K and Janis VPF-700 for the measurement from 700 K to 240 K, both with the sample in vacuum. For the pyroelectric measurements, the poling procedure was performed by field-cooling the sample with an electric field of 1.8 kV/cm down to 10 K using a Janis CCS-150 cryostat. The sample was then short-circuited for one hour. Pyroelectric current and temperature data were taken at 3 s intervals while the cryogenic refrigerator and heater have been both turned off, allowing the natural warm-up of the cryostat.

III. RESULTS AND DISCUSSION

The pyroelectric coefficient p may be written according to the following equation:[14]

$$p(T) = \frac{i}{A\left(\frac{\partial T}{\partial t}\right)}. \quad (1)$$

Here, T is the absolute temperature, A the sample area in m^2, and t is the time in seconds. The pyroelectric coefficient p as a function of temperature obtained from the short-circuit pyroelectric current i (see inset) is shown in Fig. 1. It is important to remark, in view of the fact that we are using a polycrystalline sample, that the pyroelectric current measured is the component in the direction of the electrodes. It may be composed of components of polarization in all directions. The electrical polarization in the b-axis that has been found to drive a transition to a paraelectric state is probably dominant for temperatures below 40 K. Near 175 K, we believe that the main contribution to the polarization comes from the

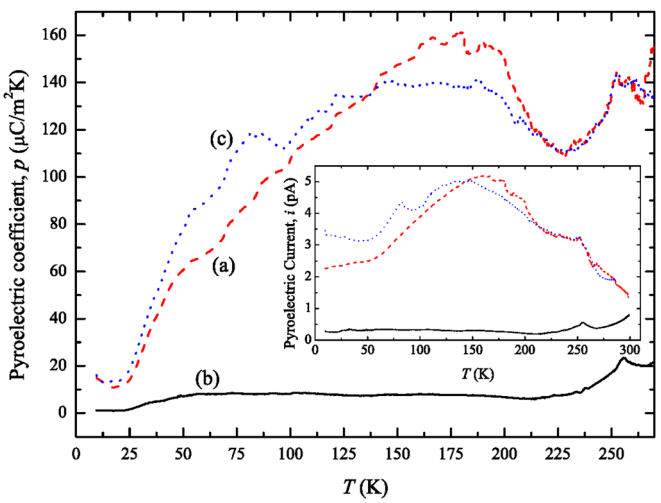

FIG. 1. (Color online) (a) Pyroelectric coefficient vs T; (b) pyroelectric coefficient vs T performed after the experiment shown in (a) without polarization; (c) pyroelectric coefficient vs T performed after the experiment shown in (b) with the same polarization of experiment (a). Inset: pyroelectric current vs T.

a-axis, in agreement with the data of pyroelectric effect reported in Ref. 12, already mentioned. A contribution from the c-axis is not totally excluded, in view of the increasing behavior of that component of the dielectric constant reported by Golovenchits *et al.*[15] For a single crystal of $EuMn_2O_5$, the same authors have found a broad maximum (130 K–170 K) in the dielectric constant with the applied field along the c-axis direction.

After the measurement shown in Fig. 1(a), a second run to measure the pyroelectric current has been done without any electrical polarization field. In Fig. 1(b), the pyroelectric coefficient of an almost completely depolarized sample is shown. Then, in order to confirm this pyroelectric current above 50 K, an experiment similar to the first described in Fig. 1(a), with the sample polarized at the same temperature and using the same value of electric field, was performed (Fig. 1(c)). Although not exactly equal, because we have not started with zero polarization and some small differences could also show up in the natural warming, Fig. 1(c) confirms the pyroelectric behavior that we have observed in Fig. 1(a). The pyroelectric currents are shown in the inset. From curves (a) and (c), one can observe features in some temperatures. We can find coincident temperatures coming from magnetic data. Garcia-Flores *et al.*[16] have reported dc-magnetic susceptibility (χ) measurements in the range 2 K to 800 K. Performing a fit of the data with a diamagnetic (χ_0) and a Curie-Weiss ($C/(T-\Theta_{CW})$) contribution, they have obtained $\Theta_{CW} = -253$ K. Plotting $(\chi - \chi_0)^{-1}$ *versus* T, they show that, below this temperature, the data deviates from the paramagnetic behavior due to magnetic correlations. They emphasize that the large ratio $|\Theta_{CW}|/T_N = 6.3$ points toward magnetic frustration. The temperature derivative of $(\chi - \chi_0)^{-1}$ also reveals other features: a maximum around 65 K and a minimum around 160 K. Observing the pyroelectric coefficient of Fig. 1, a step can be seen in curves (a) and (c) around 65 K and a maximum around 160 K in curve (c) besides the maximum observed in curves (a), (b), and (c) around 250 K. In this way, we are tempted to conclude that the magnetic data of Ref. 16 and the pyroelectric coefficient shown in Fig. 1 suggest a connection between magnetic behavior and electric polarization in $BiMn_2O_5$ at temperatures above the temperature of the antiferromagnetic transition.

In Fig. 2, dielectric constant, ε', in the range 1–11 kHz is shown for several temperatures. The low temperature data is in agreement with those reported in the literature for other RMn_2O_5 samples, if we assume that it has contributions from the three directions. The dielectric constant at low temperature along the a- and c-axis is smaller than that along the b-axis.[1,7] Assuming the a- and c-axis dielectric constant values around 10 K of 15 and the b-axis dielectric constant to be 25, a mean value of 18 for our polycrystalline sample is obtained, which is in good agreement with experimental data. Besides, for low temperatures, a tendency to a frequency independent value at high frequencies is observed in Fig. 2(a). There is a tendency to a decrease in the dielectric constant value around 38 K, which can be understood as a decrease in the contribution of the b-axis dielectric constant to the total dielectric constant due to the

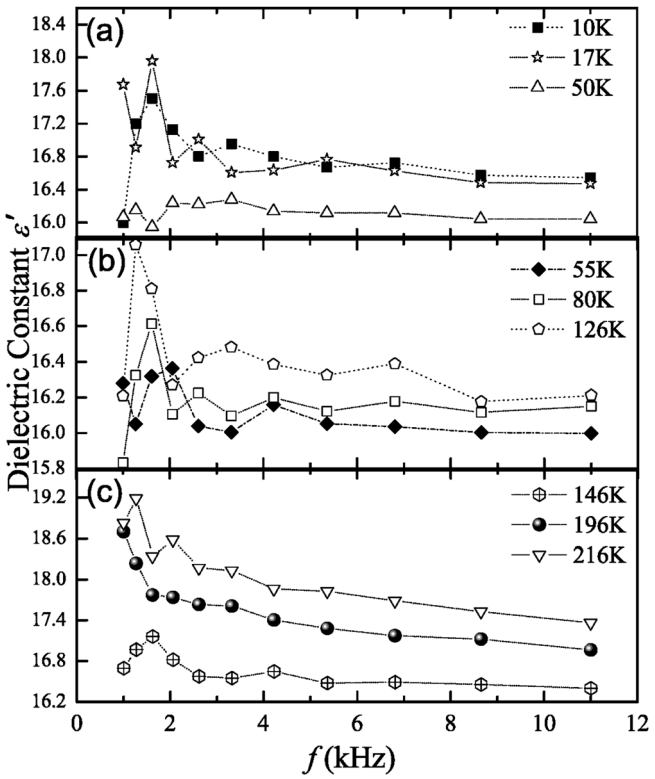

FIG. 2. Dielectric constant ε' vs f at several temperatures: (a) 10 K, 17 K, and 50 K; (b) 55 K, 80 K, and 126 K; (c) 146 K, 196 K, and 216 K.

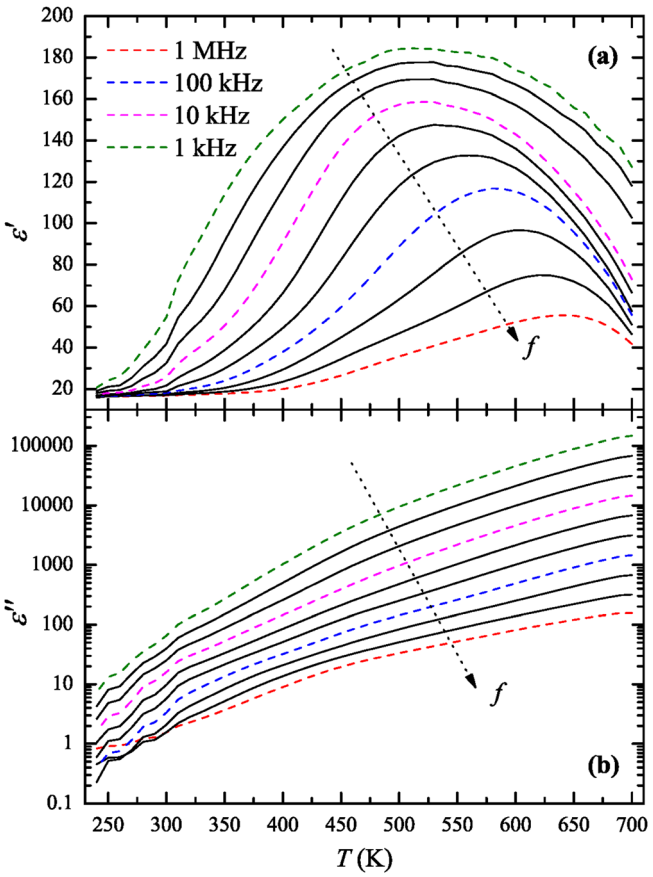

FIG. 3. (Color online) Real and imaginary parts of the dielectric constant from 240 K to 700 K.

ferroelectric-paraelectric phase transition for that direction. In Figs. 2(b) and 2(c), we can see that the dielectric constant starts to increase again and becomes more and more frequency dependent. In order to carefully study this frequency behavior, we have performed measurements in the range from 100 Hz to 1 MHz and from 700 K to 240 K. The real and imaginary parts of the dielectric constant as a function of temperature are displayed in Figs. 3(a) and 3(b), respectively. Although, in Fig. 3(a), a broad maximum is observed for all the frequencies shown, no maximum is observed in Fig. 3(b) for the same frequencies. This behavior for the imaginary part is due to the conductivity contribution, in addition to the dielectric loss. In Fig. 4, the conductivity is displayed as a function of frequency for several temperatures. For the highest temperature shown, 700 K, the conductivity is almost frequency independent, suggesting a dc behavior. The 300 K and 250 K curves show two frequency dependencies in different ranges that could suggest contributions from the dielectric loss, in addition to the conductive process. The peak in the dielectric loss has also been attenuated and shifted to higher temperatures upon doping the ferroelectric ceramic $PbBi_2Nb_2O_9$ (PBN) with Ba to yield the relaxor $Pb_{0.8}Ba_{0.2}Bi_2Nb_2O_9$.[17]

The frequency dependent broad maximum in Fig. 3(a) in the dielectric constant is clearly seen, suggesting relaxor behavior. Several models have been used to explain the relaxor behavior, most of them inspired in those used to explain the behavior of spin glass systems.[18,19] The relaxor behavior is attributed to existence of polar nanoregions (PNR), with the mechanisms of their formation not completely understood yet.[20,21] One approach is that the relaxor crystal tends to be ferro- or antiferroelectric at low temperatures, but the quenched disorder prevents the transition and the PNR appear. Within this context, the PNR are originated from the local phase fluctuations, forming islands embedded into the paraelectric matrix below the Burns temperature.[22] The polydispersion of size domains is known to cause a broadening of the relaxation times, τ, around a mean value ($\tau_{min} \leq \tau \leq \tau_{max}$),[23] which then reflects in the dielectric constant, as proposed by Courtens.[24] Other models assume the

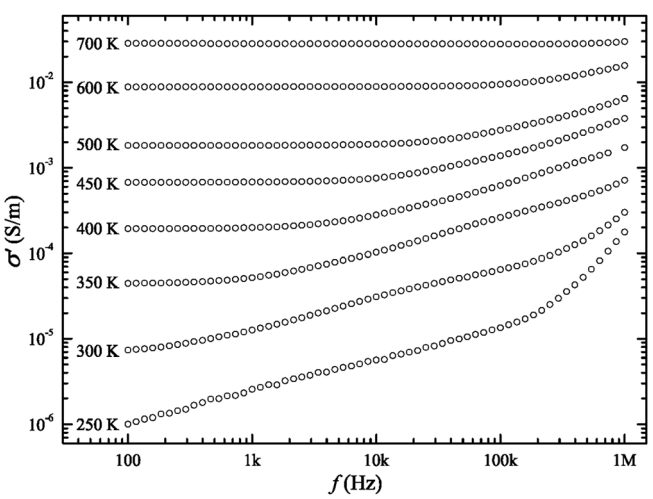

FIG. 4. Real part of the complex conductivity from 100 Hz to 1 MHz for several temperatures.

transition to occur in all regions of the crystal, which is so composed of low symmetry nanodomains separated by domain walls.[25] Different approaches[26,27] have been used to express the distribution of transition temperatures. The relaxor character can be induced by doping, as can be seen in Bi-doped $SrTiO_3$.[28]

In Ref. 15, a frequency dispersion of the dielectric constant was also observed along the *c*-axis in a single crystal of $BiMn_2O_5$ and a relaxor behavior has been proposed. However, a detailed study of the relaxor behavior could not be appropriately done, due to the few measured points of frequency and narrow temperature range. In a recent article, Lin *et al.*[29] have addressed this problem again, using polycrystalline samples of $BiMn_2O_5$ and measuring dielectric constant in a broad temperature (123 K to 523 K) and frequency (1 Hz to 10 MHz) ranges. They also have found evidence of relaxor behavior, but ruled out this possibility, since the peak temperature obeyed the Arrhenius behavior rather than the Vogel-Fulcher relation. However, our measurements in the range from 700 K to 240 K could be fitted with the Vogel-Fulcher relation for temperatures below 570 K and with Arrhenius relation above that temperature.

In Fig. 3(a), one can define T_m as the temperature in which the maximum of $\varepsilon'(T)$ occurs for each frequency. In Fig. 5, we plot ln*f* as a function of T_m. For lower frequencies, ln*f* versus T_m can be well fitted by the Vogel-Fulcher relation,[30]

$$f_{VF} = f_{0VF} \exp\left(\frac{-E_{VF}}{k_B(T_m - T_f)}\right). \quad (2)$$

Here, f_{0VF} is the saturation frequency for the flipping of the embedded polar nanoregions, E_{VF} is the activation energy related to this relaxation process, and T_f is the temperature in which the thermal flips of the polar domains freeze into a polarizable state, thus shifting their relaxation times τ toward

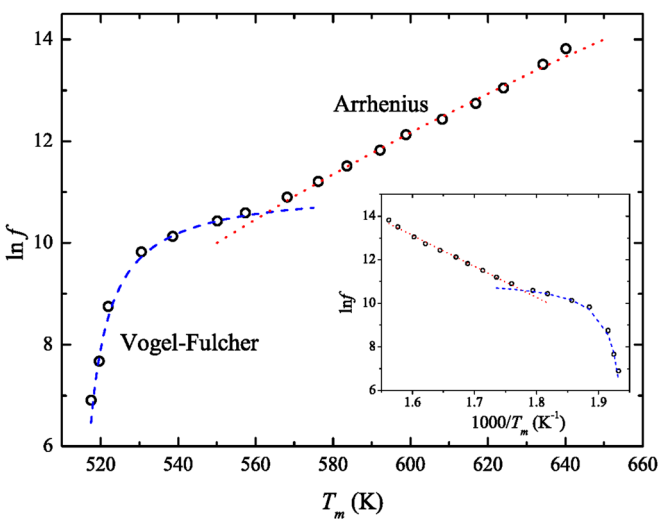

FIG. 5. (Color online) ln*f* *vs* T_m, clearly depicting the change in behavior around $T_m = 565$ K. Empty circles: experimental data; dotted line: high-frequency behavior adjusted with an Arrhenius-like relaxation process; dashed line: low-frequency behavior adjusted with the Vogel-Fulcher relation for relaxors. Inset: the same data seen as a function of the reciprocal of temperature.

macroscopic values.[31,32] The fitting yielded $f_{0VF} = 66.2$ kHz, $E_{VF} = 2.2$ meV, and $T_f = 512$ K. Above 570 K, an Arrhenius-like behavior can be observed, according to the following relation:

$$f_{AR} = f_{0AR} \exp\left(\frac{-E_{AR}}{k_B T_m}\right), \quad (3)$$

where f_{0AR} is a pre-exponential factor related to the maximum relaxation frequency for the paraelectric phase and E_{AR} is the activation energy for the charge carrier hopping. For this situation, we found $f_{0AR} = 4.76 \times 10^{15}$ Hz and $E_{AR} = 1.24$ eV. These parameters reveal the differences in dynamics for each of the compounding phases.[14] In fact, this paraelectric phase still contains some small polar clusters, and the Burns temperature is possibly attained above 700 K.

The frequency $f_{0AR} = 4.76 \times 10^{15}$ Hz obtained from the Arrhenius fitting is characteristic of electronic contribution, which extends from 10^{15}–10^{17} Hz at all temperatures in relaxors.[20] The frequency obtained from the Vogel-Fulcher fitting $f_{0VF} = 66.2$ kHz is smaller than the values reported in most relaxor systems. In $BaBi_4Ti_3Fe_{0.5}Nb_{0.5}O_{15}$ ceramics,[33] ($T_f = 558$ K, $f_{0VF} = 6.5 \times 10^8$ Hz) it is interesting to observe that, for similar values of freezing temperature, the frequency is four orders of magnitude larger than that we have found in $BiMn_2O_5$ ceramics. In films of $Sr_{1-1.5x}Bi_xTiO_3$ ($x = 0.04$, $E_{VF} = 2$ meV, $f_{0VF} = 2 \times 10^9$ Hz), for similar values of E_{VF}, a much larger frequency is observed.[34] In the typical relaxor system, $PbMg_{1/3}Nb_{2/3}O_3$ (PMN) ($E_{VF} = 40.7$ meV, $f_{0VF} = 10^{12}$ Hz, $T_f = 291$ K),[35] the very high value of the frequency has raised controversies about the physical meaning of this parameter.[36,37] In (1-x)$Pb(Mg_{1/3}Nb_{2/3})O_3$-x$Bi(Zn_{1/2}Ti_{1/2})$ (PMN-xBZT), the increase in the x content from 0.10 to 0.15 has decreased by one order of magnitude the value of f_{0VF}.[38] Nevertheless, the frequency we have found in $BiMn_2O_5$ ceramics is closer to the ideal situation of an infinite relaxation time at the freezing temperature. Besides, there is a relationship between the increase in the relaxation time and the increase in the volume of the PNR.[18] For PMN, Viehland *et al.*[39] discuss that a volume increase around 20% would imply a change in relaxation of four orders of magnitude. In this way, we can speculate that large volume PNRs are formed in $BiMn_2O_5$ ceramics below the freezing temperature. The effect of the high electric conductivity in the real part of the dielectric constant can also be seen in the Arrhenius behavior for high values of T_m shown in Fig. 5, rather than the Vogel-Fulcher shown for lower temperatures. It seems to indicate that high quality samples with high resistivities at high temperatures would shift the range of validity of the Vogel-Fulcher relation to higher temperatures.

We have assumed a connection between polarization and magnetic order from the data obtained from the pyroelectric coefficient measured until room temperature, but the true paramagnetic behavior starts around 250 K and the dielectric constant measurements have shown a relaxor behavior with a freezing temperature $T_f = 512$ K. Since there is no more magnetic order at these temperatures, a possible origin of this behavior comes from the BiO_8 contribution. Granado *et al.* in Ref. 13 have stressed that the major

difference of $BiMn_2O_5$, compared to the other RMn_2O_5, is the largely distorted BiO_8 cage, which has been ascribed to the electron lone pair. This lone pair mechanism of polarization has been seen in $BiMnO_3$ and $BiFeO_3$.[40] In both, the ferroelectric state is observed above room temperature with transitions to the paraelectric state around 760 K[41] and 1143 K,[42] respectively. For single crystals of $BiFeO_3$, values of polarization typical of normal ferroelectrics ($60\ \mu C/cm^2$) have been observed at room temperature with large values of room temperature electrical resistivity.[43] Shaldin *et al.*[44] have reported, for single crystals of $BiFeO_3$ showing high electric conductivity above 200 K, pyroelectric coefficients in the range 120 K–160 K with a maximum value of 1.2×10^{-4} C/m^2K around 140 K. This value is very similar to the maximum value of 1.6×10^{-4} C/m^2K that we have found around 160 K for our $BiMn_2O_5$ sample. For optimized $BiFeO_3$ ceramic samples, Yao *et al.*[45] have reported a room temperature pyroelectric coefficient value of 0.9×10^{-4} C/m^2K. For the same samples, they have observed at room temperature (P-E) hysteresis loops (electric field up to 1500 V/cm) with remnant values of polarizations up to $13.2\ \mu C/cm^2$. The sample quality seems to be of fundamental importance to make possible the observation of all the ferroelectric characteristics. Disorder will give rise to relaxor behavior in $BiMn_2O_5$ ceramics, and typical Arrhenius behavior is observed as the sample becomes more conductive with the increase of the temperature. However, signatures of ferroelectric behavior can still be observed, even if the sample does not have a very high resistivity.

IV. CONCLUSIONS

In this work, we have shown that, in a polycrystalline $BiMn_2O_5$ sample, a broad curve of depolarization current has been observed in the whole studied temperature range, from 10 K to 300 K, from which the pyroelectric coefficient has been obtained. The possibility of this ferroelectric behavior to be connected with magnetic correlations above the Néel temperature is discussed. A frequency dependent dielectric constant studied in the range 240 K to 700 K has revealed relaxor behavior, following Vogel-Fulcher law below 560 K with a freezing temperature at $T_f = 512$ K. This high temperature ferroelectric behavior is attributed to the Bi^{3+} in the distorted BiO_8 cage.

ACKNOWLEDGMENTS

The authors warmly acknowledge very interesting discussions and the support provided by Dr. Eduardo Granado. I. Fier and L. Walmsley are indebted to Dr. Dante Luis Chinaglia for technical support. This work was partially supported by Brazilian agencies Fapesp, CNPq, and CAPES.

[1]N. Hur, S. Park, P. A. Sharma, S. Guha, and S.-W. Cheong, Nature **429**, 392 (2004).
[2]N. Hur, S. Park, P. A. Sharma, S. Guha, and S.-W. Cheong, Phys. Rev. Lett. **93**, 107207 (2004).
[3]A. Inomata and K. Kohn, J. Phys. Condens. Matter **8**, 2673 (1996).
[4]Y. Noda, H. Kimura, M. Fukunaga, S. Kobayashi, I. Kagomyia, and K. Kohn, J. Phys. Condens. Matter **20**, 434206 (2008).
[5]J. W. Kim, S. Y. Haam, Y. S. Oh, S. Park, S.-W. Cheong, P. A. Sharma, M. Jaime, N. Harrison, J. H. Han, G.-S. Jeona, P. Coleman, and K. H. Kim, Proc. Natl. Acad. Sci. U.S.A. **37**, 8106 (2009).
[6]M. Fukunaga, K. Nishihata, H. Kimura, Y. Noda, and K. Kohn, J. Phys. Soc. Jpn **77**, 094711 (2008).
[7]M. Fukunaga, Y. Sakamoto, H. Kimura, and Y. Noda, J. Phys. Soc. Jpn **80**, 014705 (2011).
[8]K. Noda, M. Akaki, T. Kikshi, D. Akahoshi, and H. Kuwahara, J. Appl. Phys. **99**, 08S905 (2006).
[9]Y. J. Choi, C. L. Zhang, and S.-W. Cheong, Phys. Rev. Lett. **105**, 097201 (2010).
[10]L. M. Volkova and D. V. Marinin, J. Phys. Condens. Matter **21**, 015903 (2009).
[11]G. S. Geon, J.-H. Park, J. W. Kim, K. H. Kim, and J. H. Han, Phys. Rev. B **79**, 104437 (2009).
[12]I. D. Zhitomirskii, N. E. Skorokhodov, A. A. Bush, O. I. Chechernikova, V. F. Chuprakov, and Y. N. Venevstev, Sov. Phys. Solid State **25**, 550 (1983).
[13]E. Granado, M. S. Eleotério, A. F. García-Flores, J. A. Souza, E. I. Golovenchits, and V. A. Sanina, Phys. Rev. B **77**, 134101 (2008).
[14]M. Lines and A. M. Glass, *Principles and Applications of Ferroelectrics and Related Materials* (Clarendon, Oxford, 1979).
[15]E. I. Golovenchits, V. A. Sanina, and A. V. Babinskii, J. Exp. Theor. Phys. **85**, 156 (1997).
[16]A. F. Garcia Flores, E. Granado, H. Martinho, R. R. Urbano, C. Rettori, E. I. Golovenchits, V. A. Sanina, S. B. Oseroff, S. Park, and S.-W. Cheong, Phys. Rev. B **73**, 104411 (2006).
[17]H. Du, Y. Li, H. Li, X. Shi, and C. Liu, Solid State Commun. **148**, 357 (2008).
[18]R. Pirc, R. Blinc, and V. Bobnar, Ferroelectrics **370**, 203 (2008).
[19]M. Delgado, E. V. Colla, P. Griffin, M. B. Weissman, and D. Viehland, Phys. Rev. B **79**, 140102 (2009).
[20]A. A. Bokov and Z.-G. Ye, J. Mater. Sci. **41**, 31 (2006).
[21]F. HuiQing and K. E. ShanMing, Sci China, Ser. E: Technol. Sci. **52**, 2180 (2009).
[22]G. Burns and F. Dacol, Phys. Rev. B **28**, 2527 (1983).
[23]Z. Kutnjac, C. Filipic, A. Levstik, and R. Pirc, Phys. Rev. Lett. **70**, 4015 (1993).
[24]E. Courtens, Phys. Rev. B **33**, 2975 (1986).
[25]Y. Imry and S.-K. Ma, Phys. Rev. Lett. **35**, 1399 (1975).
[26]C.-S. Hong, S.-Y. Chu, C.-C. Tsai, and W.-C. Su, J. Alloys Compd. **509**, 2216 (2011).
[27]M. Correa, A. Kumar, and R. S. Katiyar, Appl. Phys. Lett. **91**, 082905 (2007).
[28]C. Ang, Z. Yu, P. Lunkenheimer, J. Hemberger, and A. Loidl, Phys. Rev. B **59**, 6670 (1999).
[29]Y. Q. Lin, Y. J. Wu, X. M. Chen, S. P. Gu, J. Tong, and S. Guan, J. Appl. Phys. **105**, 054109 (2009).
[30]H. Vogel, Phys. Z. **22**, 645 (1921).
[31]A. E. Glazunov and A. K. Tagantsev, Appl. Phys. Lett. **73**, 856 (1998).
[32]S. Saha and T. P. Sinha, J. Phys. Condens. Matter **14**, 249 (2002).
[33]S. Kumar and K. B. R. Varma, Solid State Commun. **147**, 457 (2008).
[34]O. Okhay, A. Wu, P. M. Vilarinho, and A. Tkach, J. Appl. Phys. **109**, 064103 (2011).
[35]L. E. Cross, Ferroelectrics **151**, 305 (1994).
[36]S. Ke, H. Fan, and H. Huang, Appl. Phys. Lett. **97**, 132905 (2010).
[37]J. Macutkevic, J. Banys, and R. Grigalaitis, Appl. Phys. Lett. **98**, 016101 (2011).
[38]H. N. Tailor, A. A. Bokov, and Z.-G. Ye, "Freezing of polarization dynamics in relaxor ferroelectric (1-*x*)$Pb(Mg_{1/3}Nb_{2/3})O_3$-*x*$Bi(Zn_{1/2}Ti_{1/2})O_3$ solid solution," Curr. Appl. Phys. (in press).
[39]D. Viehland, S. J. Jang, L. E. Cross, and M. Wuttig, J. Appl. Phys. **68**, 2916 (1990).
[40]S.-W. Cheong and M. Mostovoy, Nature Mater. **6**, 13 (2007).
[41]T. Kimura, S. Kawamoto, I. Yamada, M. Takano, and Y. Tokura, Phys. Rev. B **67**, 18041 (2003).
[42]J. M. Moreau, C. Michel, R. Gerson, and W. J. James, J. Phys. Chem. Solids **32**, 1315 (1971).
[43]D. Lebeugle, D. Colson, A. Forget, M. Viret, P. Bonville, J. F. Marucco, and S. Fusil, Phys. Rev. B **76**, 024116 (2007).
[44]Y. V. Shaldin, S. Matyjasik, and A. A. Bush, Crystallogr. Rep. **52**, 123 (2007).
[45]Y. Yao, B. Ploss, C. L. Mak, and K. H. Wong, Appl. Phys. A **99**, 211 (2010).